Thermochimica Acta, 91 (1985) 223–234
Elsevier Science Publishers B.V., Amsterdam – Printed in The Netherlands

KINETICS OF THE REHYDRATION OF SODIUM SULPHIDE DEHYDRATED IN SITU, UNDER FORMATION OF ITS PENTAHYDRATE

JAN Y. ANDERSSON, JOAN DE PABLO * and MICHEL AZOULAY

Department of Physical Chemistry, The Royal Institute of Technology, S-100 44 Stockholm (Sweden)

(Received 21 March 1985)

ABSTRACT

Using thermogravimetry and X-ray powder diffractometry under controlled water vapour pressure, the kinetics and mechanism of the reaction between water vapour and sodium sulphide dehydrated in situ were studied in the pressure range 3–20 Torr. Both thermogravimetry and X-ray powder diffractometry pressure jump measurements indicate that the rehydration process can only take place via a dihydrate intermediate. The sorption reaction is thus shown to proceed in two steps, which are just the reverse of the dehydration process

$Na_2S + 2H_2O\,(g) \rightarrow Na_2S \cdot 2H_2O$

$Na_2S \cdot 2H_2O + 3H_2O\,(g) \rightarrow Na_2S \cdot 5H_2O$

Kinetic measurements under isothermal and isobaric conditions at four different temperatures (50.7, 54.7, 59.7 and 64.7°C) show an almost linear dependence between temperature and pressure for the overall reaction $\tilde{0} \rightarrow \tilde{2} \rightarrow \tilde{5}$. Reaction rates were found to depend only on the sample geometry. The linear relationship is easily interpreted in terms of a simple heat transfer control process.

INTRODUCTION

The reaction mechanism of the dehydration of sodium sulphide pentahydrate to an essentially anhydrous form has recently been investigated [1]. It is found that:

(i) The reaction proceeds in two steps, (1_D) and (2_D), via an intermediate phase, which has been identified as a somewhat divariant sodium sulphide dihydrate, according to the following reactions

$$Na_2S \cdot 5H_2O\,(c) \rightarrow Na_2S \cdot 2H_2O\,(c) + 3H_2O\,(g) \qquad (1_D)$$

$$Na_2S \cdot 2H_2O\,(c) \rightarrow Na_2S \cdot xH_2O\,(c) + (2 - x)\,H_2O\,(g) \qquad (2_D)$$

where $x \approx 0.2$–0.5.

* Present address: Escola Superior d'Enginiers, Industrials Catedra Quimica I, Diagonal 649, Barcelona, Spain.

0040-6031/85/$03.30

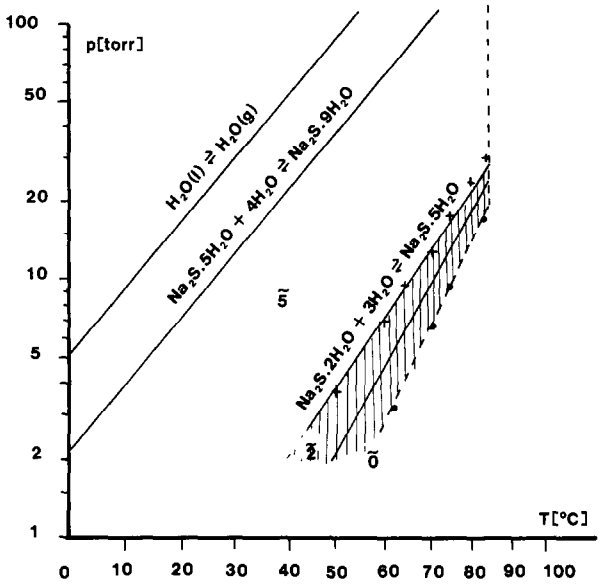

Fig. 1. Pressure/temperature diagram for the Na_2S–H_2O system: (+) equilibrium data recorded for a $\tilde{5}+\tilde{2}$ mixture; (●) onset temperatures of decomposition of $\tilde{5}$ phase, as recorded by T_c-scanning thermogravimetry. The inhibition domain for reaction (2) is shown by the hatched area.

The subscripts D and R, will henceforth denote the dehydration and the rehydration direction, respectively, of the corresponding reaction step. A number without subscript indicates the corresponding equilibrium reaction. The pentahydrate, dihydrate and anhydrous sodium sulphide phases will be denoted $\tilde{5}$, $\tilde{2}$ and $\tilde{0}$, respectively.

(ii) The stability domains of the various participating species, viz. $\tilde{5}$, $\tilde{2}$ and $\tilde{0}$, have been delimited and are depicted in Fig. 1.

(iii) Reaction (2) has been shown to possess a relatively pronounced inhibition domain as compared to reaction (1).

The sodium sulphide–water vapour system is interesting in two respects. First, the overall rehydration reaction proceeds easily to completion. Second, during successive dehydration–rehydration cycles it exhibits an exceptionally low hysteresis, although the change in water content (i.e., the mole ratio difference = 5 mol H_2O/Na_2S) of the substance during the course of the reaction is quite large. In fact, this behaviour has been practically exploited in the Tepidus chemical heat pump system [2].

It is noteworthy that complete rehydration of anhydrous or hydrated salts has been reported only for a few salt hydrate systems, such as potash alum, barium chloride, barium styphnate, copper sulphate, hexagonal calcium sulphate, lead styphnate, manganese formate, potassium carbonate, sodium sulphate and uranyl nitrate [3–17].

The present mechanistic study shows that the rehydration process pro-

ceeds just along the reverse reaction, i.e., via the $\tilde{2}$ phase (cf. Scheme 1), which is assumed to be structurally related to $\tilde{5}$ as well as to $\tilde{0}$ [1].

EXPERIMENTAL

Materials

Two different qualities of sodium sulphide $Na_2S \cdot nH_2O$, viz. reagent grade (Merck or Prolabo, crystallized, composition $n = 9$) and technical grade (ICI, flake-shaped, $n \approx 3$), were used in the experiments.

In some experiments, the reagent-grade material was further purified by recrystallization from distilled water before use [1] and its water composition was analyzed by determining its sulphide content using an iodometric titration procedure [18]. It was then confirmed that the stoichiometry corresponds to 9.0 moles H_2O per mole Na_2S. Special precautions were taken to avoid any oxidation, carbonation or hydrolysis side reactions.

In the thermogravimetric (TG) temperature scanning experiments, only unsieved, recrystallized reagent grade $Na_2S \cdot 9H_2O$ was used. The particle size of the starting material was ca 0.5–1 mm, and the initial weight was about 20 mg, which approximately corresponded to a monolayer. The $\tilde{0}$-hydrate was initially prepared in situ by drying the nonahydrate by slowly increasing the temperature at the same water vapour pressure under which the sorption was to be performed. Water contents associated with the various steps in the thermogram were inferred from the absolute weights recorded by the thermobalance according to

$$n = 13.34(m/m_9) - 4.34 \tag{3}$$

where n is the mole ratio [mol H_2O/mol Na_2S], m the sample weight and m_9 the weight of the nonahydrate used as the starting material.

In the TG kinetic experiments, both reagent and technical grade qualities were used. The former material was dried in a vacuum oven overnight, ground and sieved. The fraction 100–125 μm was selected for the experiments. The ICI flake-shaped samples were utilized either without further treatment (approximate flake dimensions: thickness, 1 mm; average diameter, 5 mm) or ground into a powder and subsequently sieved (particle size 100–125 μm). An initial weight of about 8 mg was used (with a water content corresponding to $n \approx 3$). All kinetic investigations were conducted using samples which had been subjected to several dehydration–rehydration cycles (> 2), prior to any measurement.

In the X-ray experiments a couple of grams of reagent grade nonahydrate were used. The $\tilde{5}$ and $\tilde{0}$ phases were prepared in situ in the apparatus.

Instrumentation and experimental procedure

Thermogravimetry

The thermogravimetric experiments were conducted using a McBain quartz spring balance under controlled, pure water vapour pressure. Hereafter, the constraint pressure and temperature in the apparatus are denoted T_c and p_c, respectively. The balance has already been described [1,4]. This apparatus was intended both for temperature scanning and isothermal experiments using the pressure jump technique. The sensitivity of the balance was 0.05 mg for weight change measurements, which gives an absolute accuracy of about 0.03 in the mole ratio n (defined above). The equipment was initially thoroughly evacuated and degassed.

In the temperature scanning experiments, two different scanning rates, viz. 3 and 12°C h^{-1}, were utilized.

In the cycling experiments, hydrogen gas at a partial pressure of 20 Torr was present in the apparatus in order to suppress continuous degradation.

In the pressure jump experiments the reaction was started by applying an instant pressure increase, performed by switching between two evaporators kept at different temperatures. Just prior to a pressure jump, $\tilde{5}$-hydrate was dehydrated to $\tilde{0}$-hydrate at 70°C and 5.7 Torr. The temperature T_c was then set to 50, 55, 60 or 65°C, and after attainment of thermal equilibrium the pressure jump was performed. The final pressures were selected in the interval 6–20 Torr.

X-ray diffraction equipment

The two types of X-ray powder diffractometers utilized have previously been described in detail [1].

(i) A θ–2θ diffractometer equipped for operation in a pure water vapour atmosphere at constant pressure and temperature [19]. The temperature of the sample compartment is controlled by using circulating thermostatted water. The water vapour pressure may be changed from one pressure to another by means of two evaporators, one containing distilled water and the other saturated calcium chloride solution, both at 20°C.

(ii) A combined θ–θ diffractometer and thermobalance [20]. This equipment allowed for simultaneous recordings of X-ray diffractograms and sample weight. It operated at controlled water vapour pressure.

RESULTS

Temperature scanning

Thermogravimetric studies

The influence of pressure and temperature on the sorption process, as recorded by linearly decreasing the temperature, is illustrated in Fig. 2 at

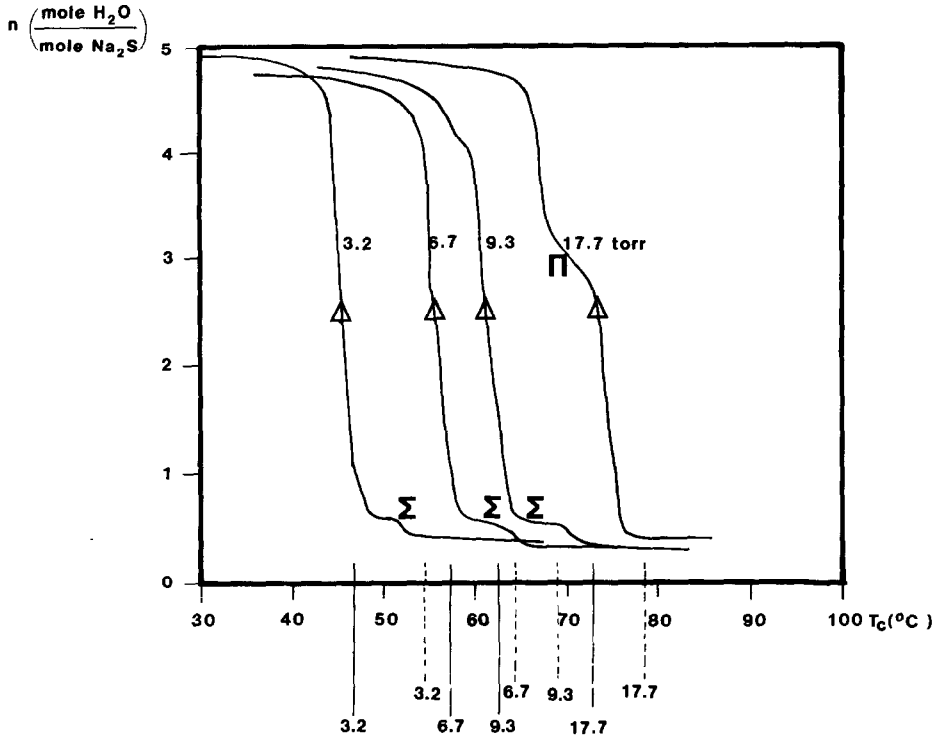

Fig. 2. Thermograms for rehydration of the $\tilde{0}(\tilde{2})$ phase, recorded at four p_c settings: 3.2, 6.7, 9.3 and 17.7 Torr. Temperature range: ca. 80–40°C; scanning rate: 3°C h^{-1}. Equilibrium temperatures of reactions (1) (———) and (2) (-----) (taken from ref. 1) are inserted in the T_c-axis. Σ and Π denote plateaus.

various pressures, p_c, viz. 3.2, 6.7, 9.3 and 17.7 Torr. At the highest pressure, a distinct plateau (Π) appears at a mole ratio n (see Experimental section) approximately equal to 3. However, at the lower pressures, this feature is absent in the thermograms which are apparently similar, although the derivatives exhibit a slight change in slope in the neighbourhood of this n value. The latter effect was observed to vary, probably due to slight differences in the prehistory of the $\tilde{0}(\tilde{2})$ material. (The $\tilde{0}$ phase contains small amounts of $\tilde{2}$, cf. Discussion.) Moreover, it is noteworthy that at such low pressures, cooling the $\tilde{0}(\tilde{2})$ compound leads to another type of plateau (Σ), at which a small water uptake ($\Delta n \approx 0.2$) occurs. Thereby, no water sorption takes place until the temperature approaches the equilibrium temperature of reaction (1). The equilibrium temperatures of this reaction as reported elsewhere [1], are included in the figure.

The thermograms recorded at $p_c = 6.7$ Torr for successive dehydration–rehydration cycles almost coincide (see Fig. 3). The dehydration and rehydration branches reach a limit shape already during the second cycle. A peculiar feature of the dehydration branch is the small shoulder appearing

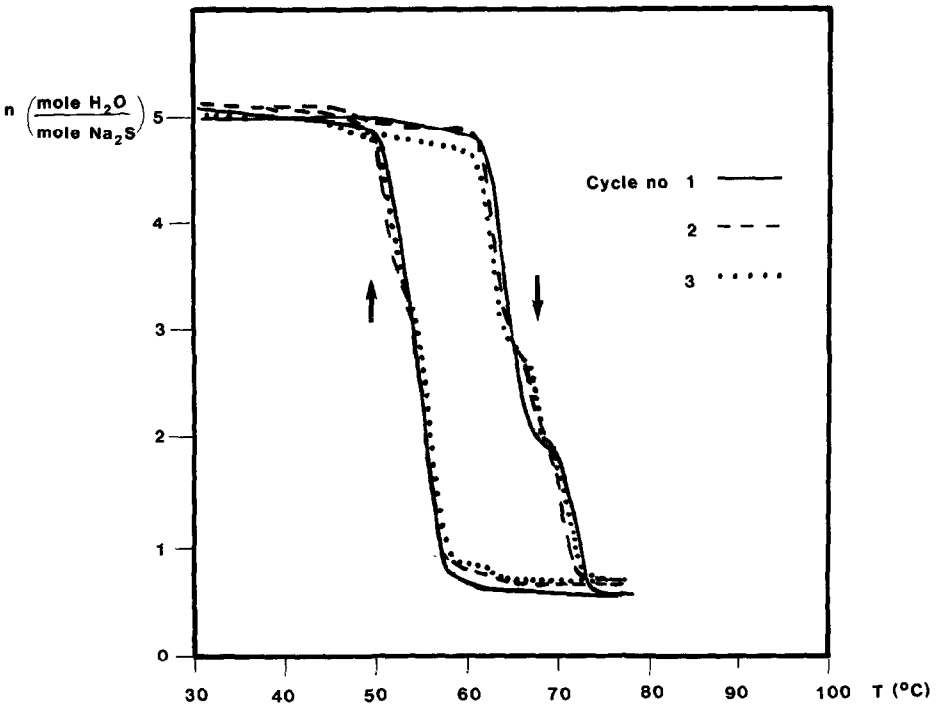

Fig. 3. Thermograms for successive dehydration–rehydration cycles of sodium sulphide, at $p_c = 6.7$ Torr. Hydrogen pressure = 20 Torr.

after one cycle at a mole ratio $n = 3$. A second feature is that the water content of the $\tilde{0}(\tilde{2})$ phase increases significantly with the cycle number.

Only when the $\tilde{2}$ phase is incompletely dehydrated (i.e., $n = 1.2$) does subsequent rehydration lead to the characteristic $\tilde{2}$ plateau observed during dehydration.

X-ray investigations

In these experiments the angle-scanning method was utilized to monitor the phases occurring during the course of a rehydration. The sample compartment was cooled down freely from ~ 75°C. When initiating a run, as shown in Fig. 4, the 18.3° line of the $\tilde{2}$ phase increases [1] concomitantly with a relatively small decrease in the 19.5° line intensity, where the latter describes the $\tilde{0}$ phase. Then the latter line disappears very abruptly, while those associated with $\tilde{5}$ gradually rise. It should be noted that during rehydration of the $\tilde{0}(\tilde{2})$ phase, $\tilde{2}$ is always observed, at least as an intermediate. Moreover, the diffractogram of $\tilde{2}$, in addition to the 18.3°, line contains the 15.0° line, which emerges at lower temperatures. These two lines have been tentatively attributed to two different but closely related structures, analogous to what is observed for order–disorder transitions.

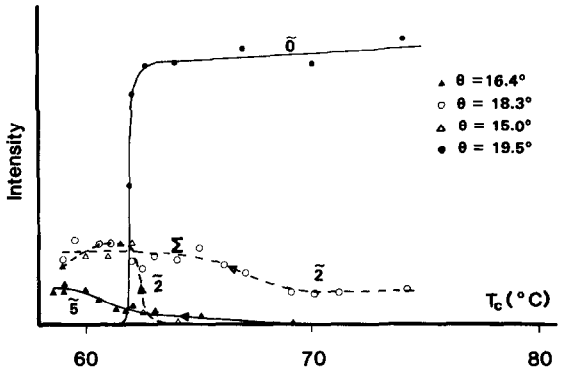

Fig. 4. Intensities of prominent X-ray diffraction lines of a $Na_2S \cdot nH_2O$ sample (θ values are given), vs. T_c at $p_c = 8$ Torr. Scanning rate ca. 10°C h^{-1} (free cooling). The symbols adjacent to the curves denote the different hydrate species. The intensity axis refers to diffraction peak height (arbitrary scale).

Kinetic investigations at isothermal and isobaric conditions

Measurement of progress curves at isobaric conditions

Typical rehydration pressure jump curves are presented as Young plots in Fig. 5, where two typical water content vs. reduced time, τ, curves are shown, for different particle geometries, viz. flakes and powder. The curves presented represent samples of technical quality. The sample quality did not seem to influence the shape of the curves. These curves are similar in the

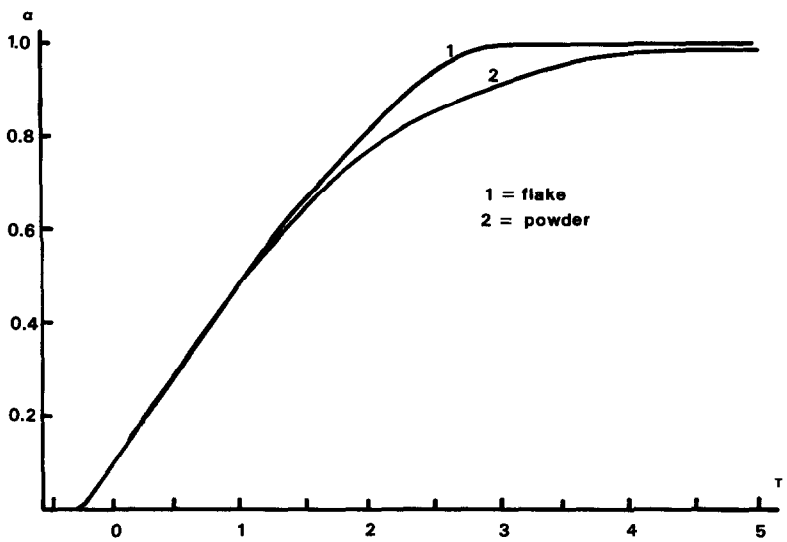

Fig. 5. Pressure jump progress curves showing the extent of reaction α vs. reducted time, τ, for two different sample geometries.

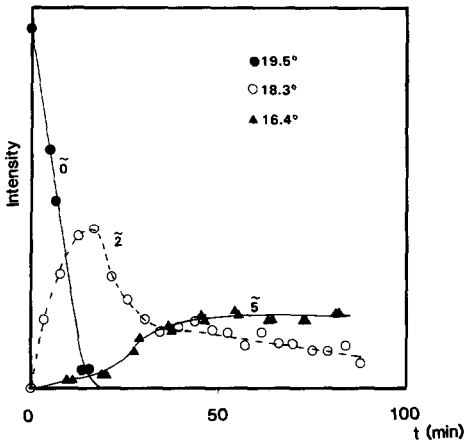

Fig. 6. Intensities of prominent X-ray diffraction lines of an $Na_2S \cdot nH_2O$ sample vs. time, as recorded in a pressure jump experiment.

sense that both of them lack an induction period and both possess linear initial sections.

The results obtained from an X-ray pressure jump run are presented in Fig. 6. The $\tilde{2}$ phase clearly participates as an intermediate state in the rehydration to pentahydrate. It should be stressed that for this particular experiment the $\tilde{5}$ phase was dehydrated to completion under vacuum conditions, prior to the experiment.

Reaction rate isotherms: the influence of pressure and particle geometry

The reaction rate, defined as the slope dn/dt [mol H_2O/(mol $Na_2S \cdot$ s)] of the initial linear sections of the n vs. time curves, are plotted against pressure at four different temperatures in Fig. 7. The investigated pressure range was 3–20 Torr. The dependence of the reaction rate upon pressure is nearly linear throughout. Furthermore, it appears from the family of curves obtained that the reaction kinetics of the flakes are slower than those of the powder. In the latter case it was also found that the reaction rates were fairly independent of the sample quality, i.e., technical vs. pro analysis, in spite of the different origin of these two samples. The sample geometry was found to be the only parameter, besides p_c and T_c, which substantially influenced the reaction rate.

In order to account for the influence of pressure on the observed rates, it was assumed, as an initial approximation, that complete heat transfer control applies to the system, i.e., mass transfer and chemical processes are unimportant. This is reasonable, due to the low heat transfer coefficient between particles and the ambient low-pressure atmosphere [21,22]. In this case only heat conduction in the gas phase contributes significantly to the total heat transfer, since radiation and convection effects as well as heat

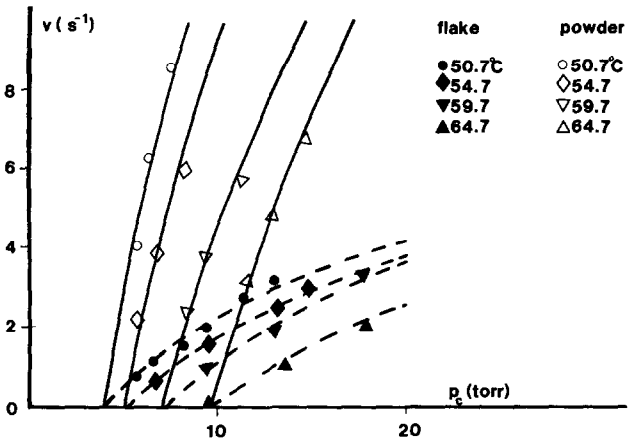

Fig. 7. Reaction rate isotherms, (dn/dt) [mol H_2O/(mol Na_2S·s)], vs. p_c, at different T_c-values and for two sample geometries, viz. powder (———) and flake (-----).

conduction in the solid may be neglected in this temperature range. In other words, this means that for spherical particles eqn. (4) holds.

$$Nu = (hd)/\lambda = 2 \leftrightarrow h = 2\lambda/d \tag{4}$$

where Nu = Nusselt number, h = heat transfer coefficient, d = particle diameter (m) and λ = heat conductivity of water vapour (ca. 0.02 W m^{-1} K^{-1}). Moreover, the local equilibrium hypothesis is assumed, i.e., the surface of the particle is assumed to be in thermal equilibrium with the vapour phase layer in immediate contact with it.

The above assumptions, together with the approximation that the whole particle has rapidly reached a steady state temperature, i.e., the heat produced outweighs the heat outflow, give

$$v(p_c, T_c) = \frac{dn}{dt} = \frac{12M\lambda[T_c - T_e(p_c)]}{\Delta H d^2 \rho \times 10^9} \tag{5}$$

where n = the mole ratio H_2O/Na_2S, t = time (s), M the molar weight of Na_2S (78 g mol^{-1}), ΔH the heat of reaction (60.6 kJ mol^{-1} H_2O) and ρ the particle density (ca. 1.9 g cm^{-3}). The reaction heat was assumed to equal that of reaction (1). T_e is the equilibrium temperature of reaction (1) at the pressure p_c. For the purpose of checking this model, the experimental data of the flake-shaped sample were first fitted to eqn. (5), in order to roughly estimate some equivalent particle radius [21]. The calculated radii, $d_{calc} = 0.9 \pm 0.1$ mm, compare favourably with those measured experimentally, i.e., average thickness $d_{exp} = 1$ mm (see Materials section). In contrast, when applying the same model to the powdered sample, a poor concordance was found, i.e., $d_{calc} = 0.40 \pm 0.05$ mm, instead of $d_{exp} = 0.11 \pm 0.02$.

DISCUSSION

Characterization of the in situ prepared $\tilde{0}(\tilde{2})$ phase

It is well known that the experimental conditions under which a salt hydrate is dehydrated to a lower hydrated form, substantially influence the subsequent rehydration to the initial salt hydrate. The dehydration rate and p–T conditions are among the important factors [10,23]. The reasons for this are that the crystallinity, the number of remaining nuclei, the porosity and the surface area of the sample are affected by these.

Thermogravimetry shows that when $\tilde{5}$ is dehydrated to the $\tilde{0}(\tilde{2})$ phase, the latter still contains 0.2–0.9 mol H_20/mol Na_2S (cf. Fig. 2). It was found [1] that the water content depends largely on the rate of this in situ dehydration, higher water contents being obtained at higher rates (see ref. 1). X-ray powder diffraction shows the occurrence of $\tilde{2}$ in the $\tilde{0}(\tilde{2})$ phase. Therefore, the measured water content of the $\tilde{0}(\tilde{2})$ phase may be attributed to the presence of $\tilde{2}$ together with some adsorbed water (at least $n = 0.2$). The interesting question is then why the $\tilde{2}$ species is found far from its stability domain (cf. Fig. 1). Although this finding is not completely understood, it may be suggested that the apparently metastable existence of $\tilde{2}$ stems from a favourable structural relationship between the $\tilde{2}$ and $\tilde{0}$ lattices [1,24].

The total amount of transient $\tilde{2}$ species is presumably low at higher dehydration rates, which implies a final lower content of $\tilde{2}$ in the $\tilde{0}(\tilde{2})$ phase. The change in water content with the rate of the previous dehydration can be explained in the following way. When the dehydration is slow, the $\tilde{2}$ phase has enough time to crystallize in an ordered form which undergoes a phase transformation to the $\tilde{0}$ phase with some difficulty. When the dehydration is fast, however, $\tilde{2}$ is obtained only as a fairly disordered transient phase which readily loses water, yielding $\tilde{0}(\tilde{2})$ with smaller amounts of $\tilde{2}$.

The mechanism and kinetics of the rehydration of sodium sulphide

The pressure jump X-ray diffraction studies show unambiguously the participation of $\tilde{2}$ as an intermediate in the rehydration from $\tilde{0}$ to $\tilde{5}$, which is thus similar to the dehydration reaction (see Scheme 1).

The equilibrium pressures for reactions (1) and (2), inserted in the T_c-axis of Fig. 1 [1], suggest that the Σ plateau results from the $\tilde{0} \rightarrow \tilde{2}$ transformation. However, the reaction slows down before the conversion to $\tilde{2}$ is complete. Furthermore, it should be mentioned that the Σ plateau falls within the inhibition region of reaction (2) (cf. Fig. 1). This kind of partial rehydration is found for many other anhydrous or hydrated salts, e.g., lithium hydroxide [25], manganese oxalate and other examples given in ref. 10. This effect is generally believed to be due to the formation of an impenetrable layer of rehydrated product around the crystallites, which

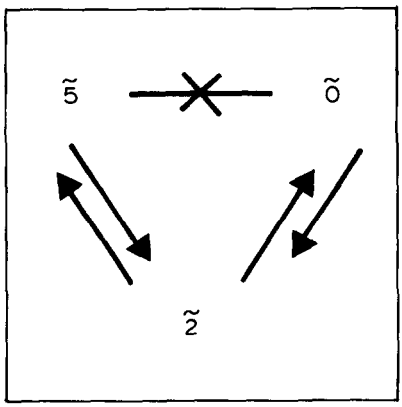

Scheme 1. Mechanism of the overall transformation $\tilde{0} \rightleftarrows \tilde{5}$.

impedes the reaction. This is consistent with the experimental finding that the onset temperatures of the Σ-plateaus are close to the estimated equilibrium temperatures of reaction (2) [1]. A further increase in water content is not detected until the equilibrium temperature of reaction (1) is reached. Additional evidence for this interpretation is given by the temperature scanning X-ray results shown in Fig. 4, where the 18.3° curve also displays a Σ plateau. The figure shows clearly that no substantial disappearance of $\tilde{0}$ occurs before the building up of $\tilde{5}$.

As was mentioned above, the thermogram at the highest pressure level differs in the sense that the Σ plateau is absent, while a Π plateau appears at a higher water content. At such high temperatures, the extent of inhibition of reaction (1) should be comparatively low (see Fig. 1). Consequently, the rehydration of $\tilde{0}$ to $\tilde{2}$ can proceed easily, at least at temperatures lower than the equilibrium temperature of reaction (1). The occurrence of the Π plateau at such a high water content as $n \approx 3$ is not fully understood. However, the existence of mixed crystals between $\tilde{5}$ and $\tilde{2}$ cannot be excluded, especially because of their presumably similar structures.

The reaction rate isotherms are readily interpreted using eqn. (5), which seems to be a good approximation for the flake-shaped sample. However, for the powdered material the model seems to be somewhat less satisfactory, taking into account the fact that the particles are in fairly close contact with each other. This results in a smaller contact area with respect to the gas phase, and thus to less efficient heat transfer [21].

ACKNOWLEDGEMENTS

This work has been financed by the National Swedish Board for Technical Development (STU), The Swedish Council for Building Research (BFR) and

The Swedish Natural Science Research Council. We are grateful to Professor G. Bertrand, Laboratoire de Recherches sur la Réactivité des Solides (LRS), Dijon, France for his interest in this work. The X-ray diffraction experiments have been carried out at the LRS. We should thank LRS for their hospitality during the stay of one of us (J.Y.A.).

REFERENCES

1 J.Y. Andersson and M. Azoulay, J. Chem. Soc., Dalton Trans., in press.
2 G. Wettermark (Ed.), Proc. Int. Seminar on Thermochemical Energy Storage, Stockholm, 1980, Swedish Council for Building Research.
3 A. Bielanski and F.C. Tompkins, Trans. Faraday Soc., 46 (1950) 1072.
4 J. Andersson, M. Azoulay and J. de Pablo, Thermochim. Acta, 70 (1983) 291.
5 F.C. Tompkins and D.A. Young, Trans. Faraday Soc., 52 (1956) 1245.
6 G. Bertrand, M. Lallemant and G. Watelle-Marion, J. Inorg. Nucl. Chem., 36 (1974) 1303.
7 M.C. Ball and L.S. Norwood, J. Chem. Soc., Faraday Trans. 1, 69 (1973) 169.
8 M. Trollier and B. Guilhot, Bull, Soc. Chim. Fr., (1977) 1.
9 T.B. Flanagan, Can. J. Chem., 44 (1966) 2941.
10 R.C. Eckhardt, P.M. Fichte and T.B. Flanagan, Trans. Faraday Soc., 67 (1971) 1143.
11 M.A. Stanish and D.D. Perlmutter, AIChE J., 30 (1984) 56.
12 S. El and D. Hamad, Thermochim. Acta, 17 (1976) 85.
13 R.M. Dell and S.W. Weller, Trans. Faraday Soc., 55 (1959) 2203.
14 P. Barret and R. Thiard, C.R. Acad. Sci., 260 (1965) 2823.
15 N. Gerard, G. Watelle-Marion and A. Thriell-Sorel, Bull. Soc. Chim. Fr., 5 (1967) 1788.
16 B. Beden, A. Cointot, M.J. Croissant and G. Valensi, Kinetics in Heterogeneous Chemical Systems, Elsevier, Amsterdam, 1975.
17 M.L. Franklin and T.B. Flanagan, J. Chem. Soc., Dalton Trans., (1972) 192.
18 B. Eriksson, R. Rådeström and L. Sjöström, SCAN-Forsk No. 315, Research Rep., Swedish Forest Products Research Laboratory, Stockholm, Sweden, and references therein.
19 N. Gerard and G. Watelle-Marion, Bull. Soc. Chim. Fr., (1963) 2631.
20 N. Gerard, J. Phys. Educ., 7 (1974) 509.
21 J.Y. Andersson, H. Bjurström, M. Azoulay and B. Carlsson, J. Chem. Soc., Faraday Trans., in press.
22 R.B. Bird, W.E. Stewart and E.N. Lightfoot, Transport Phenomena, Wiley, New York, 1960.
23 H.W. Quinn, R.W. Missen and G.B. Frost, Can. J. Chem., 33 (1955) 546.
24 E. Zintl, A. Harder and B. Dauth, Z. Electrochem., 40 (1934) 588.
25 J.Y. Andersson, J. de Pablo and M. Azoulay, to be published.